AJNR

Central Skull Base Osteomyelitis in Patients without Otitis Externa: Imaging Findings

Patrick C. Chang, Nancy J. Fischbein and Roy A. Holliday

AJNR Am J Neuroradiol 2003, 24 (7) 1310-1316
http://www.ajnr.org/content/24/7/1310

AJNR Am J Neuroradiol 24:1310–1316, August 2003

Central Skull Base Osteomyelitis in Patients without Otitis Externa: Imaging Findings

Patrick C. Chang, Nancy J. Fischbein, and Roy A. Holliday

BACKGROUND AND PURPOSE: **Skull base osteomyelitis typically arises as a complication of ear infection in older diabetic patients, involves the temporal bone, and has *Pseudomonas aeruginosa* as the usual pathogen. Atypical skull base osteomyelitis arising from the sphenoid or occipital bones without associated external otitis occurs much less frequently and initially may have headache as the only symptom. The purpose of this study was to review the clinical and MR imaging features of central skull base osteomyelitis.**

METHODS: **We retrospectively reviewed MR images obtained in six patients with central skull base osteomyelitis. No patient had predisposing external otitis or osteomyelitis of the temporal bone.**

RESULTS: **All of our patients presented with headache, no external ear pain, and cranial nerve deficits. Five of six patients had a predisposition to infection, and the erythrocyte sedimentation rate was elevated in the five patients in whom it was checked. In each case, the diagnosis was delayed until MR imaging demonstrated central skull base abnormality, and the diagnosis was then confirmed with tissue sampling. The most consistent imaging findings were clival bone marrow T1 hypointensity and preclival soft tissue infiltration. Five of six patients were cured with no recurrence of skull base infection over a 2–4-year follow-up period.**

CONCLUSION: **In the setting of headache, cranial neuropathy, elevated erythrocyte sedimentation rate, and abnormal clival imaging findings, central skull base osteomyelitis should be considered as the likely diagnosis. Early tissue sampling and appropriate treatment may prevent or limit further complications such as intracranial extension, empyema, or death.**

Typical cases of skull base osteomyelitis are initiated by ear infections in older diabetic patients, with *Pseudomonas aeruginosa* as the usual pathogen (1, 2). Atypical skull base osteomyelitis occurs much less frequently and does not begin with otitis externa. It is centered on the sphenoid and occipital bones rather than the temporal bone. Patients initially may have headache as the only symptom, with cranial neuropathies occurring later (3). The diagnosis is difficult to make clinically and therefore is often delayed. Recognition of characteristic imaging findings such as diffuse clival hypointensity on T1-weighted MR images due to bone marrow infiltration (4, 5) is crucial to making a timely diagnosis. Our purpose was to describe the characteristic clinical presentation and MR imaging findings of central skull base osteomyelitis in patients without otitis externa to facilitate recognition of this unusual condition and thereby encourage prompt tissue sampling and institution of appropriate medical and, possibly, surgical intervention.

Methods

The medical records and imaging studies of six patients identified as having central skull base osteomyelitis without otitis externa were retrospectively reviewed. Cases were identified over the course of 7 years, from 1993 to 2000. Individuals with typical skull base osteomyelitis ("necrotizing otitis externa") and those whose condition began in the ear and then simply extended to the central skull base as a complication of the primary process were excluded from this study group. Patients were all male and ranged in age from 13 to 72 years, with a mean age of 40 years. We obtained institutional review board approval to perform this study.

All patients were examined with MR imaging before biopsy and treatment. Imaging included sagittal, axial, and coronal T1-weighted images, axial fast spin-echo T2-weighted images with fat saturation, and axial and coronal postcontrast T1-weighted images with fat saturation. Images were assessed qualitatively with regard to skull base marrow signal intensity, presence of abnormal soft tissue, and signal intensity of any abnormal soft tissue.

Received November 26, 2002; accepted after revision February 10, 2003.

From the Department of Radiology, University of California, San Francisco, School of Medicine, San Francisco, CA (P.C.C., N.J.F.) and the Department of Radiology, New York Eye and Ear Infirmary, New York, NY (R.A.H.)

Address reprint requests to Nancy J. Fischbein, M.D., Department of Radiology, University of California, San Francisco School of Medicine, Box 0682, 505 Parnassus Avenue, San Francisco, CA 94143.

TABLE 1: Clinical characteristics of patients with atypical central skull base osteomyelitis

Patient (no.)	Age (y)/ Sex	Risk Factors	Biopsy Performed	Organism Isolated	Cranial Neuropathies
1	50/M	Diabetes mellitus, chronic sinusitis	CT fine needle aspiration	*Eikenella corrodens*	VI, IX, X, XII
2	13/M	Diabetes mellitus	Sphenoidotomy	*Staph aureus, Serratia marcescens, Aspergillus niger*	V2, VI, VII, VIII, IX, X, XI, XII
3	38/M	HIV positive, replacement steroids	Autopsy	*Aspergillus fumigatus*	VI, VII
4	72/M	Diabetes mellitus	CT fine needle aspiration	*Pseudomonas aeruginosa*	IX, X
5	33/M	Chronic sinusitis	Sphenoidotomy	Group C *Streptococcus*	VI
6	35/M	Diabetes mellitus, steroids	Craniotomy	*Streptococcus milleri*	III, VI, VII, IX, X, XII

TABLE 2: MR findings in atypical central skull base osteomyelitis

Patient (no.)	Abnormal SI in Clivus	Preclival ST Mass	T1 SI in Clivus	T2 SI in Clivus	Postcontrast Enhancement	ST in CS	ST in MC	IC Extension
1	Y	Y	Low	High	Y	N	N	N
2	Y	Y	Low	Heterogeneous	Y	Y*	Y	N
3	Y	Y	Low	Heterogeneous	Y	Y*	Y	Y
4	Y	Y	Low	High	Y	N	N	N
5	Y	Y	Low	High	Y	Y	Y	N
6	Y	Y	Low	High	Y	Y*	Y	Y

Note.—Signal intensity in clivus is compared with that of normal fatty marrow. SI indicates signal intensity; ST, soft tissue; CS, cavernous sinus; MC, Meckel's cave; IC, intracranial. Intracranial extension implies extension beyond CS or MC, involving dura or brain parenchyma or both.

* = associated carotid narrowing or occlusion.

Five patients underwent direct tissue sampling: in two patients, CT-guided fine-needle aspiration (FNA) of preclival soft tissue masses was performed, and in three patients, open biopsy of soft tissue or bone was performed. Biopsy specimens were delivered to microbiology for culture and to pathology for histologic analysis. Five patients had an erythrocyte sedimentation rate (ESR) test performed. An HIV-positive patient received a presumptive diagnosis on the basis of MR imaging appearance, and this was subsequently confirmed at autopsy. All patients were treated with broad-spectrum empiric antibiotics, and in some cases antifungal and antituberculous drugs, until cultures and antibiotic susceptibility results were returned.

Two patients underwent combined ^{99m}technetium-^{67}gallium scanning at the time of initial diagnosis and at follow-up. Two patients underwent follow-up MR imaging at our institution.

Results

Patients' clinical characteristics are summarized in Table 1. Each of the patients presented with headache and without evidence of external otitis, acute otitis media, or mastoiditis. All patients had cranial neuropathy by the time they presented to our institution, with cranial nerve (CN) VI palsy present in five patients and CN IX, X, and XII palsy present in three patients (Table 1). Two patients had a history of chronic sinusitis, four had underlying diabetes mellitus, and one was HIV positive. ESR was tested in five patients, all of whom had elevated values ranging from 21–75 mm/h, with a mean of 34 mm/h. Only patient 2 had documented fever, and two patients (patients 1 and 6) had elevated white blood cell (WBC) counts of 13.2×10^9/L and 15.3×10^9/L; mean WBC count for all patients was 10.8×10^9/L. No patient had positive blood cultures.

In all cases, MR imaging of the skull base was abnormal (Table 2). The most consistent MR finding was regional or diffuse clival hypointensity on T1-weighted images relative to normal fatty marrow, which was noted in all patients. There were also signs of pre- and paraclival soft tissue infiltration with obliteration of normal fat planes or even frank soft tissue masses (Fig 1) in all patients. Four patients had abnormal soft tissue in the cavernous sinus, and three of these patients also had internal carotid artery narrowing, slow flow, or occlusion as assessed on spin-echo images by the size of the vessel and the presence or absence of a normal flow void. Because MR angiography was not performed in most patients, we could not distinguish slow flow from occlusion with confidence. T2 signal intensity of the clivus was diffusely high in four patients and heterogeneously high in two patients, and postgadolinium enhancement was seen in all patients. Two patients had abnormal dural enhancement, and one patient (6) had abnormal leptomeningeal enhancement as well as signal intensity abnormality in the adjacent brain parenchyma (Fig 2), presumably reflecting a local cerebritis or venous ischemia. The three patients with CN XII palsy had abnormal marrow signal intensity around the hypo-

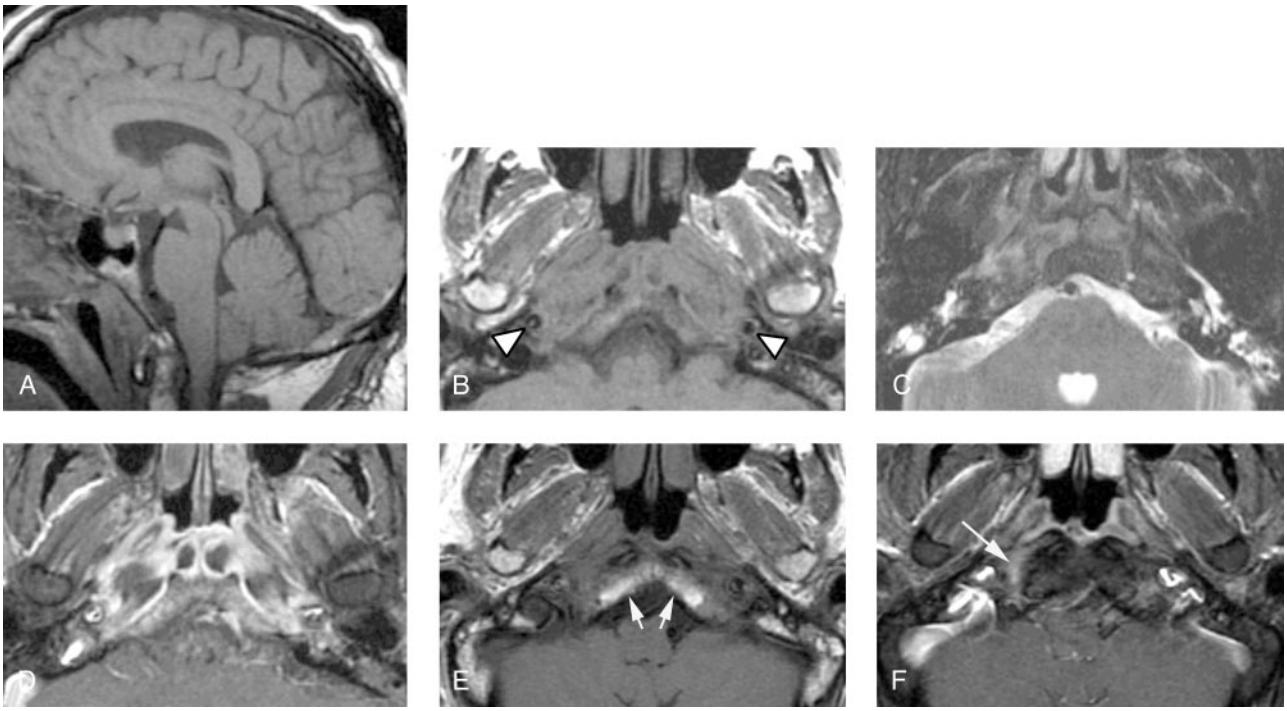

FIG 1. Patient 1, a 50-year-old man presenting with a severe headache, diplopia, and the sensation of a "thick" tongue.

A, Sagittal T1-weighted image (600/11/2 [TR/TE/NEX]) demonstrates abnormally low signal intensity in the inferior clivus.

B, Axial T1-weighted image (600/11/2) demonstrates abnormal soft tissue isointense to muscle infiltrating submucosally within the nasopharyngeal soft tissues, extending posteriorly to abut the carotid arteries (*arrowheads*), and replacing the normal hyperintense fatty marrow within the lower clivus.

C, Axial T2-weighted fast spin-echo image with fat saturation (4000/102/2) demonstrates mildly increased signal intensity within the infiltrated soft tissue as compared with normal muscle. In addition, there is fluid in the mastoid air cells and middle ear cavities bilaterally, presumably related to Eustachian tube dysfunction or obstruction or both.

D, Contrast-enhanced axial T1-weighted spin-echo image with fat saturation (600/11/2) demonstrates moderately intense enhancement of the infiltrative soft tissue. Some areas of nonenhancement may represent areas of infarcted or necrotic muscle.

E, Axial T1-weighted spin-echo image (600/11/2) from a follow-up MR examination 16 months after the initial study demonstrates normalization of clival signal intensity (*white arrows*), as well as considerable reduction in bulk of the previously noted abnormal pre- and paraclival soft tissue.

F, Contrast-enhanced axial T1-weighted spin-echo image with fat saturation (600/11/2) from the same follow-up examination demonstrates marked reduction of enhancement, with a normal appearance to the nasopharynx and prevertebral muscles. An ill-defined area of linear enhancement just at and anterior to the hypoglossal canal on the right (*arrow*) is likely extending along the course of the hypoglossal nerve. Of note, this patient's hypoglossal palsy has persisted despite resolution of all other symptoms.

glossal canal as well as abnormal soft tissue infiltrating adjacent fat planes, and their tongues showed evidence of acute or subacute denervation change.

Three patients had simple fluid collections in the mastoid air cells or middle ear cavity or both that were visible on imaging studies. This fluid was thought to be secondary to Eustachian tube dysfunction in the setting of abnormal nasopharyngeal submucosal inflammatory soft tissue or reactive adenoidal hypertrophy or both rather than a reflection of temporal bone infection, because no patients had symptoms referable to the external or middle ear or mastoid. All patients also had either active sphenoid sinus disease or a history of sphenoid sinus disease. Patient 1 (Fig 1) had undergone prior functional endoscopic sinus surgery with resolution of his inflammatory mucosal disease, whereas patients 2–6 had imaging evidence of varying degrees of mucosal abnormality.

Diagnosis was made by sampling of preclival soft tissues by CT-guided FNA in two patients (Fig 3) and by surgical biopsy in three patients. An organism was successfully recovered in all five patients (Table 1). A biopsy was not performed in the case of the HIV-positive patient, but an autopsy was performed. The osteomyelitis was bacterial in four cases, mixed bacterial and fungal in one case, and fungal in one case.

Five of the six patients responded well to 6 weeks of targeted intravenous antibiotic therapy, with resolution of headache and normalization of WBC count and ESR. Our HIV-positive patient had an undetectable CD4 count, as well as fungal sinusitis complicated by skull base osteomyelitis, and he subsequently died of massive brain infarction due to fungal invasion and occlusion of his left internal carotid artery and basilar artery. All five surviving patients had persistent cranial nerve dysfunction despite successful treatment of their infection, although some patients had improvement or resolution of particular deficits. No recurrences of central skull base infection were observed in the follow-up period of 2–4 years for the five patients who survived.

Two patients underwent baseline nuclear medicine studies, with a positive technetium-gallium study in

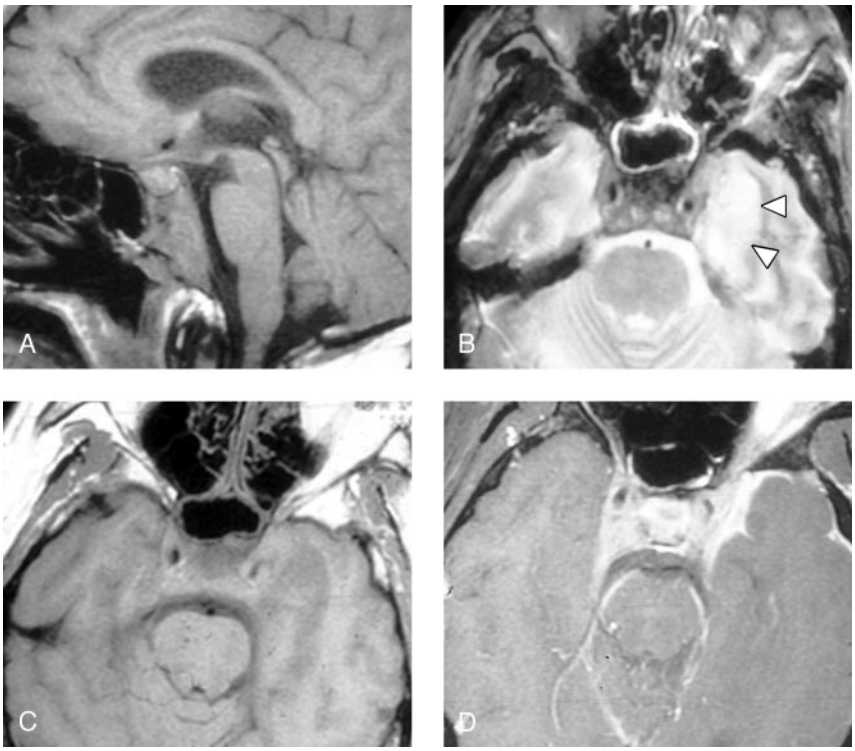

FIG 2. Patient 6, a 35-year-old man presenting with headache and bilateral deficits of CN III, VI, VII, X, and XII. The patient had been previously treated with steroids and oral antibiotics for paranasal sinus inflammatory disease.

A, Sagittal T1-weighted MR image (600/11/2) shows diffuse low signal intensity in the clivus, with prominence of preclival soft tissue and thickening of the retroclival dura.

B, Axial T2-weighted spin-echo image (2500/80/0.75) demonstrates mild circumferential mucosal thickening in the sphenoid sinus. Abnormal low signal intensity soft tissue is present within the cavernous sinuses bilaterally, and there is mild narrowing of the left cavernous carotid flow void. High signal intensity in the left temporal lobe (*arrowheads*) is present, presumably due to either focal cerebritis or localized venous ischemia/infarction.

C, Axial T1-weighted spin-echo image (600/11/2) demonstrates abnormal soft tissue in the cavernous sinuses bilaterally and swelling of the left temporal lobe with poor definition of adjacent cerebral sulci. The left internal carotid artery appears patent but narrowed. Fat within the orbits and sphenotemporal buttresses is unremarkable.

D, Contrast-enhanced axial T1-weighted image (600/11/2) with fat saturation demonstrates dural and leptomeningeal enhancement along the anterior left temporal lobe, as well as expansion of the cavernous sinuses bilaterally and extension of abnormal enhancement along the tentorium. Apparent enhancement of the left orbital fat is secondary to a failure of fat saturation in the inferior orbit of this somewhat rotated patient. Note that the orbital fat is seen to be normal in panel *C.*

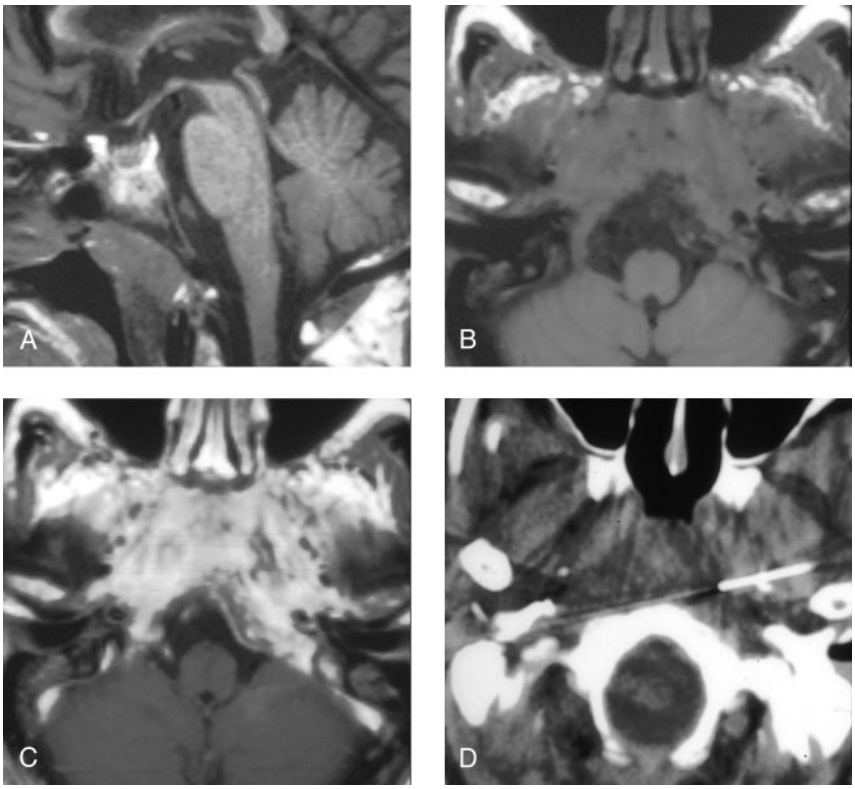

FIG 3. Patient 4, a 72-year-old man presenting with headache, dysphagia, and progressive hoarseness.

A, Sagittal T1-weighted image (600/11/2) demonstrates abnormally hypointense signal in the lower clivus.

B, Axial T1-weighted image (600/11/2) demonstrates abnormal soft tissue isointense to muscle infiltrating submucosally into the nasopharyngeal tissues, around the carotid arteries, and back to abut the abnormal clivus.

C, Contrast-enhanced axial T1-weighted image (600/11/2) demonstrates marked enhancement within the infiltrated tissue.

D, CT-guided FNA of the preclival soft tissues shows the needle tips anterior to the lower clivus.

each case. It was thought that these scans would serve as a baseline for future assessment of therapeutic response, and both patients demonstrated improvement in inflammatory changes on follow-up scans obtained at the conclusion of antibiotic therapy. Follow-up MR imaging performed at our institution was

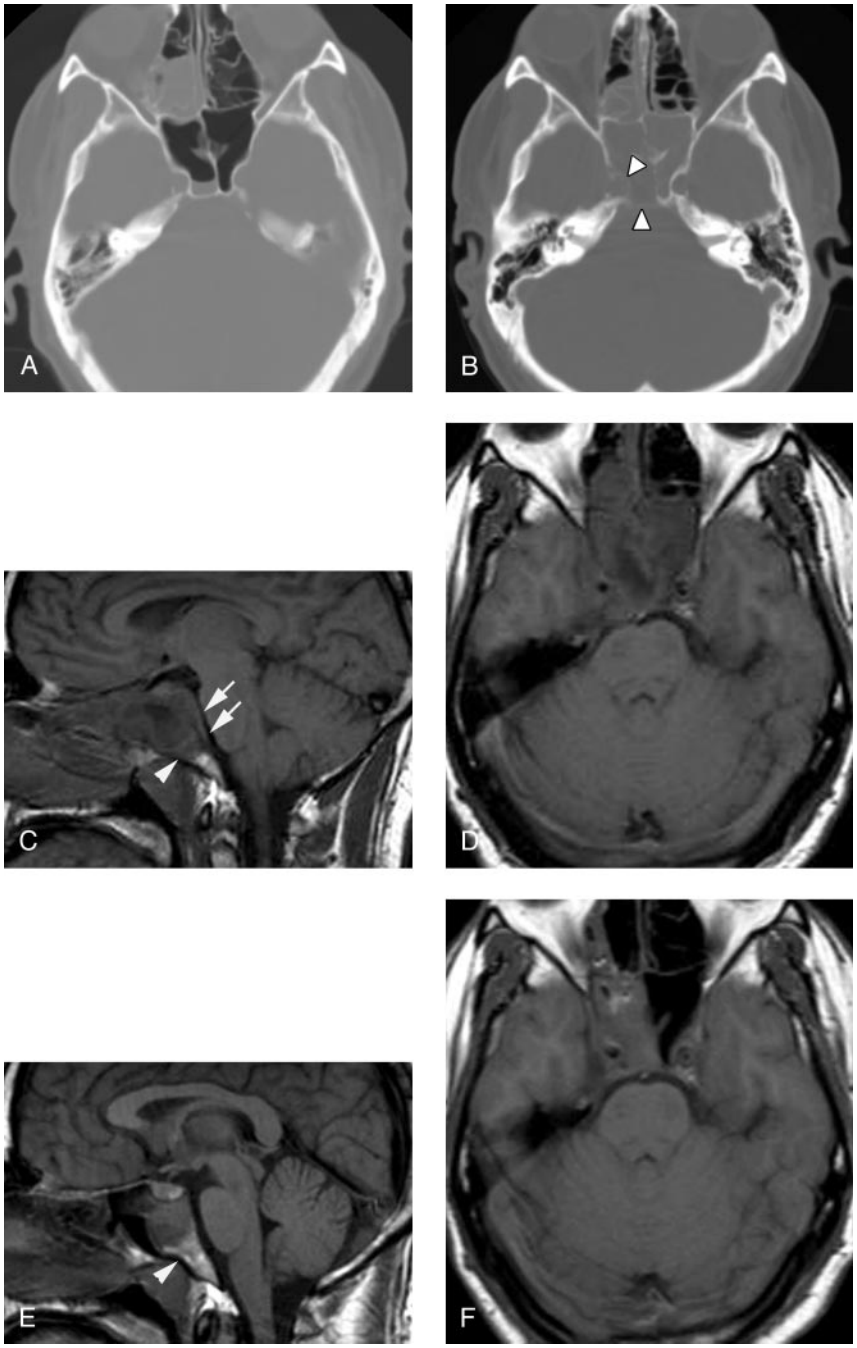

FIG 4. Patient 5, a 33-year-old man presenting with severe headache and sinus congestion.

A, Unenhanced axial CT image (bone window) demonstrates mucosal thickening in the right ethmoid sinus and an air-fluid level in the right sphenoid sinus. The bony walls of the sphenoid sinus are normal. Diagnosis of acute-on-chronic sinusitis was made and Septra and a decongestant were prescribed for the patient.

B, Three weeks later, the patient returned with continued headache and new diplopia on right lateral gaze. Unenhanced axial CT image (bone window) demonstrates segmental erosion of the bony wall of a completely opacified sphenoid sinus (*arrowheads*).

C, Sagittal T1-weighted spin-echo image (600/11/2) demonstrates abnormal hypointense signal intensity in the upper clivus (*arrowhead*) and thickening of the retroclival dura (*arrows*). The sphenoid sinus is filled with fluid and soft tissue.

D, Axial T1-weighted image (600/11/2) demonstrates abnormal soft tissue in the right cavernous sinus, with preservation of the right carotid flow void. Abnormal clival hypointensity is present, as is extensive inflammatory disease of the sphenoid and posterior ethmoid sinuses.

E, Sagittal T1-weighted spin-echo image (600/11/2) after 1 month of intravenous antibiotic therapy demonstrates normalization of signal intensity in the clivus (*arrowhead*), as well as a reduction in inflammatory sinus disease and resolution of the retroclival dural thickening.

F, Axial T1-weighted spin-echo image (600/11/2) from the same follow-up examination also demonstrates improvement in sinus disease. Abnormal soft tissue persists in the right cavernous sinus but is reduced in volume. The patient's CN VI palsy had resolved by the time of this follow-up examination.

available for only two patients. These follow-up studies demonstrated a decrease in abnormal pre- and paraclival soft tissue, as well as improvement in abnormal clival signal intensity (Figs 1 and 4).

Discussion

Osteomyelitis of the central skull base is an uncommon condition that is potentially life threatening if not promptly recognized and properly treated (1). It often presents subtly and nonspecifically with persistent headache and eventual development of cranial neuropathy. Patients with this condition seem to have a predisposition to infection because of an underlying condition such as diabetes mellitus, corticosteroid use, HIV infection, or chronic inflammatory sphenoid sinus disease.

The most common organism involved in skull base osteomyelitis arising from otitis externa is *Pseudomonas aeruginosa* (1). In these typical cases of skull base osteomyelitis, patients usually present with otitis externa, but are then found to have involvement of the marrow of the mastoid and petrous parts of the temporal bone and the adjacent soft tissues of the infratemporal fossa (6). In our series of atypical skull base osteomyelitis involving primarily the sphenoid bone, we observed only one case of *Pseudomonas*, with Gram-positive organisms being more common. Two

of our patients had an invasive fungal skull base infection caused by an *Aspergillus* species, presumably secondary to an underlying fungal sinus infection. Isolated reports of atypical skull base osteomyelitis secondary to fungal infection have previously implicated *Mucormycosis* and *Aspergillus* (7, 8).

Imaging of the skull base in the setting of cranial neuropathy and probable infection is best accomplished with MR. MR has the advantage of superior soft tissue discrimination without the beam-hardening artifacts of CT and is particularly useful for assessing soft tissue planes around the skull base and abnormalities of the medullary cavity of bone. Highly sensitive but nonspecific MR findings of osteomyelitis include marrow T1 hypointensity and T2 hyperintensity (5), imaging findings that were observed in our study. Clival enhancement can be seen with both infectious and neoplastic processes, but it should not be observed under normal circumstances. The use of fat suppression on the postgadolinium study is of course necessary to assess skull base enhancement accurately.

We noted clival marrow and preclival soft tissue abnormalities in all of our cases. It is unclear whether the preclival soft tissue abnormalities were due to direct extension of the inflammatory process inferiorly from the sphenoid sinus or whether it was an anterior extension of the process from the clivus itself. The anterior cortex of the clivus was grossly intact in all cases, but this does not preclude anterior spread of infectious organisms. Sagittal T1-weighted images of the clivus were the most useful for detecting abnormalities of the clival marrow, whereas axial T1-weighted images offered the best evaluation of the pre- and paraclival soft tissues. The coronal plane and administration of gadolinium offered the best assessment of Meckel's cave and the cavernous sinus, as well as skull base dura and inferior temporal lobes.

Processes to be considered in the clinical and imaging differential diagnosis of central skull base osteomyelitis include neoplastic, pseudoneoplastic, and nonneoplastic entities. Neoplastic processes such as squamous cell carcinoma of the head and neck, lymphoma, and hematogenous metastasis can involve the clivus, preclival soft tissues, and sphenoid sinus. Neoplasms such as squamous cell carcinoma or minor salivary tumor with skull base extension would generally result in a more focal destructive mass, rather than the diffuse infiltrative pattern observed in our cases. Lymphoma, however, could appear identical on imaging studies. Leukemia would be expected to give a more diffuse pattern of marrow involvement (ie, not only clivus, but also the calvarium and cervical spine), and would be unlikely to demonstrate the associated soft tissue changes. Nasopharyngeal carcinoma can be diffusely infiltrative but usually has an identifiable mucosal mass lesion, and the nasopharyngeal mucosa was intact in all of our cases. Elevation of the ESR would not be expected in the setting of skull base neoplasm, and this can be a helpful clinical feature in limiting the differential diagnosis.

Several other processes, including inflammatory pseudotumor, Wegener granulomatosis, other granulomatous diseases such as tuberculosis and sarcoid, fibrous dysplasia, and Paget disease can potentially mimic the imaging appearance of skull base osteomyelitis and must also be considered. Inflammatory pseudotumor and Wegener granulomatosis could demonstrate the MR findings seen in the cases presented here. Tuberculosis would be expected to be more focally destructive of bone but could certainly be a cause of central skull base osteomyelitis and could demonstrate imaging findings similar to those presented here. Sarcoidosis can affect bone and soft tissue, but the diffuse marrow abnormality and contiguous non-nodal soft tissue abnormality would be highly unusual. Fibrous dysplasia and Paget disease can result in abnormal marrow signal intensity on MR images, but they have a typical CT appearance, cause bone expansion rather than erosion, and would not be expected to have an associated soft tissue abnormality.

A tissue sampling procedure is often required for definitive diagnosis of this condition, because the imaging appearance alone is highly suggestive but nonspecific for skull base osteomyelitis. A definite diagnosis was made in two patients by CT-guided FNA of abnormal preclival tissue. For the other cases, diagnosis was made by endoscopic sphenoidotomy, open craniotomy, or, in one case, autopsy. Potentially complicating diagnosis is the fact that a low burden of infectious organisms within the clival bone or preclival soft tissues can lead to a false-negative biopsy. New modalities such as MR-guided biopsy of soft tissue surrounding the skull base may prove to be useful under these circumstances (9). In our cases, the relatively young age of most patients, the lack of any history of neoplasia, the presence of factors that predispose to infection, and signs of infection such as elevated ESR were very helpful in raising the concern for skull base osteomyelitis and indicating the need for prompt tissue sampling. It is interesting that elevated WBC count, fever, and abnormal blood cultures were remarkably absent in our patients, indicating that skull base infection should not be excluded in a patient with no fever and normal WBC count.

Other imaging techniques can help support the diagnosis of skull base osteomyelitis. Technetium scans may be helpful for initial diagnosis, although they may remain "hot" for months following resolution of infection (10). Gallium scan abnormalities have been shown to be useful to monitor response to treatment and evaluate recurrence (3). CT findings are generally unhelpful for monitoring response to treatment, because the CT scan may not even be abnormal initially or, if abnormal, may remain abnormal for as longs as 2 years after treatment (6).

Several potentially serious complications can arise as a result of skull base osteomyelitis, including cranial neuropathy, soft tissue involvement of the cavernous sinus with or without cavernous sinus thrombosis, and meningeal and brain parenchymal extension. Cranial nerve involvement is commonly seen because of the proximity of the clivus to the brain stem, basal cisterns, cavernous sinuses, and skull base foramina. A recent

study of 21 patients with combined CN VI and XII palsies implicated a process involving the clivus in 18 cases (11). We observed that cranial neuropathies resolved slowly in patients, despite successful treatment of infection. Other groups have also noted slowly resolving cranial neuropathy secondary to skull base osteomyelitis (3). MR imaging is useful to monitor response to therapy (12), and the MR marrow signal intensity in our two patients with follow-up imaging gradually reverted toward normal as their symptoms resolved. Other imaging techniques such as CT or nuclear medicine studies are unable to follow precisely the changes occurring in the clival bone marrow and surrounding soft tissue.

The abnormal soft tissue in the cavernous sinuses in four of our patients with central skull base osteomyelitis is presumably secondary to direct extension of the process from the clivus or sphenoid sinus or both. Septic cavernous sinus thrombosis is also a known complication of ethmoid or maxillary sinuses infection (13). Intracranial extension beyond just the cavernous sinuses was seen in two patients, both with dural involvement and one with both leptomeningeal and brain parenchymal involvement. Other complications of skull base osteomyelitis reported in the literature have included epidural abscess of the cervical spine as a result of spread of infection through the prevertebral space (14) and petroclival abscess (15).

Conclusion

Central skull base osteomyelitis is centered on the clivus rather than the temporal bones and presumably arises in most cases from paranasal sinus inflammatory disease rather than otitis or mastoiditis, although it may also be hematogenous in origin. Like typical skull base osteomyelitis, patients tend to be diabetic or otherwise immunocompromised, and classic signs of infection (fever, elevated WBC count, positive blood cultures) are notably absent. Our patients presented with headache and cranial neuropathy, and all had clival and preclival abnormalities on MR images, best appreciated on T1-weighted images. Once the diagnosis was suggested on the basis of clinical and MR imaging features, the diagnosis was confirmed by tissue sampling, and appropriate therapy was instituted. Follow-up MR imaging in two patients showed progressive resolution of abnormal clival and preclival signal intensity abnormalities; however, some cranial nerve deficits did persist clinically. We emphasize that this diagnosis should be considered in the setting of headache, cranial neuropathy, an elevated ESR, and abnormal clival imaging so that biopsy specimens are submitted for culture and not just for cytologic and pathologic assessment.

References

1. Chandler JR, Grobman L, Quencer R, Serafini A. **Osteomyelitis of the base of the skull.** *Laryngoscope* 1986;96:245–251
2. Mendez G, Jr., Quencer RM, Post MJ, Stokes NA. **Malignant external otitis: a radiographic-clinical correlation.** *AJR Am J Roentgenol* 1979;132:957–961
3. Grobman LR, Ganz W, Casiano R, Goldberg S. **Atypical osteomyelitis of the skull base.** *Laryngoscope* 1989;99:671–676
4. Kimura F, Kim KS, Friedman H, et al. **MR imaging of the normal and abnormal clivus.** *AJR Am J Roentgenol* 1990;155:1285–1291
5. Erdman WA, Tamburro F, Jayson HT, et al. **Osteomyelitis: characteristics and pitfalls of diagnosis with MR imaging.** *Radiology* 1991;180:533–539
6. Rubin J, Curtin HD, Yu VL, Kamerer DB. **Malignant external otitis: utility of CT in diagnosis and follow-up.** *Radiology* 1990;174:391–394
7. Lee JH, Park YS, Kim KM, et al. **Pituitary aspergillosis mimicking pituitary tumor.** *AJR Am J Roentgenol* 2000;175:1570–1572
8. Chan LL, Singh S, Jones D, et al. **Imaging of mucormycosis skull base osteomyelitis.** *AJNR Am J Neuroradiol* 2000;21:828–831
9. Kacl GM, Carls FR, Moll C, Debatin JF. **Interactive MR-guided biopsies of maxillary and skull-base lesions in an open-MR system: first clinical results.** *Eur Radiol* 1999;9:487–492
10. Seabold JE, Simonson TM, Weber PC, et al. **Cranial osteomyelitis: diagnosis and follow-up with In-111 white blood cell and Tc-99m methylene diphosphonate bone SPECT, CT, and MR imaging.** *Radiology* 1995;196:779–788
11. Keane JR. **Combined VIth and XIIth cranial nerve palsies: a clival syndrome.** *Neurology* 2000;54:1540–1541
12. Kothari NA, Pelchovitz DJ, Meyer JS. **Imaging of musculoskeletal infections.** *Radiol Clin North Am* 2001;39:653–671
13. Assefa D, Dalitz E, Handrick W, et al. **Septic cavernous sinus thrombosis following infection of ethmoidal and maxillary sinuses: a case report.** *Int J Pediatr Otorhinolaryngol* 1994;29:249–255
14. Azizi SA, Fayad PB, Fulbright R, et al. **Clivus and cervical spinal osteomyelitis with epidural abscess presenting with multiple cranial neuropathies.** *Clin Neurol Neurosurg* 1995;97:239–244
15. Hoistad DL, Duvall AJ 3rd. **Sinusitis with contiguous abscess involvement of the clivus and petrous apices: case report**. *Ann Otol Rhinol Laryngol* 1999;108:463–466